PARAMETRIC SUB-OPTIMAL H_∞ CONTROLLERS FOR AN OPTRO-MECHANICAL SYSTEM MODELED BY A TIME-DELAY 4TH ORDER SYSTEM

Guillaume Rance [1,2,3], Yacine Bouzidi [2], Alban Quadrat [2], Arnaud Quadrat [1]

[1] Safran Electronics & Defense, 100 Avenue de Paris, 91300 Massy, France.
Email: {guillaume.rance, arnaud.quadrat}@safrangroup.com
[2] Inria Lille Nord Europe, NON-A project, 40 Avenue Halley, Bat A – Park Plaza, 59650 Villeneuve d'Ascq, France. Email: {yacine.bouzidi, alban.quadrat}@inria.fr
[3] Laboratoire des Signaux et Systèmes (L2S, UMR CNRS 8506), CentraleSupélec – CNRS – Université Paris-Sud, 3 rue Joliot-Curie, 91192 Gif-sur-Yvette, France.

KEYWORDS: automatic control, robust control, time-delay systems, computer algebra, parametric controllers.

ABSTRACT:

The paper aims to study the robust stabilization of the *line of sight* of a *stabilized mirror system*. This system can be modeled by a single-input single-output time-delay system. Due to large model uncertainties, non-parametric methods are usually too conservative. Hence, we shall consider here unfixed model parameters. Using an additive decomposition, we show how to compute parametric H_∞ controllers of the time-delay model. Such a symbolic approach is interesting in the context of *adaptive control* and is illustrated throughout a simulation with an ideal parameter estimator.

1. INTRODUCTION

To stabilize the *Line Of Sight* (LOS) of high definition cameras subjected to a vibrating environment, a classical approach is to use a stabilized mirror system (see Figure 1, Chapter 5 of [1] and [2]).

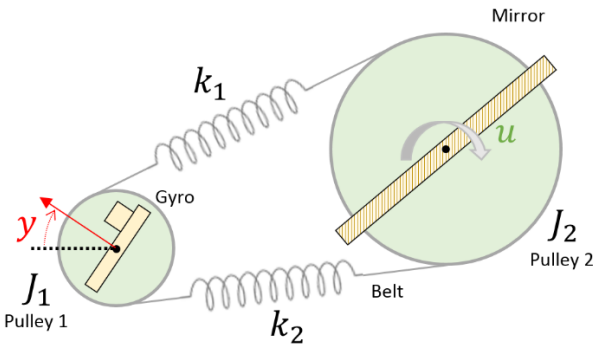

Figure 1 Stabilized Mirror System

The rotation of the mirror, oriented by motors, deflects the LOS to compensate the disturbances acting on the camera. Through a system of pulleys and belts, a gyroscope measures the orientation of the LOS, which is used to drive the mirror and stabilize the LOS by means of a feedback law.

The physical relation between the torque u and the rotational speed y (measured by the gyroscope) can be modelized by means of differential time-delay equations. A common way to represent this relation is to use a transfer function. Denoting by s the Laplace variable, the transfer function G from u to y (identified from measurements) is a single-input single-output (SISO) system defined by the product of a time-delay system and a rational 4th order system. More precisely, G is defined by

$$G := \frac{y}{u} = \frac{g}{s}\left(\frac{\frac{s^2}{\omega_0^2} + 2\,\xi\,\frac{s}{\omega_0} + 1}{\frac{s^2}{\omega_1^2} + 2\,\xi\,\frac{s}{\omega_1} + 1}\right)\left(\frac{1}{Ts+1}\right) e^{-\tau s}, \qquad \text{Eq. 1}$$

where all the parameters $\theta := (g, \xi, \omega_0, \omega_1, T, \tau)$ are real strictly positive, $0 < \xi \leq 1$ and $\omega_0 < \omega_1$. We call ω_1 the *natural modal frequency* of G.

The belts, which link the pulleys, are *highly resonating mechanical systems* [3]. Their resonating frequencies can vary with temperature. To deal with these model uncertainties, H_∞ *control techniques* [4] can be used (see [5], [6], [7]). More specifically, in this paper, we propose to use H_∞ loop-shaping robust control techniques to design a control law. These techniques were firstly introduced in [4] and then further developed, for instance, in [8] or [9]. H_∞ control is attractive in an industrial context because it provides a natural compromise between the performance and the robustness to perturbations and uncertainties of the closed-loop system.

This control problem applied to rational systems involves the resolution of an *algebraic Riccati equation* and eigenvalues calculations, which are both classically done numerically. However, [10] and [11] showed (through different ways) how to solve this problem for rational linear systems with unfixed model parameters. In [12] and [13], explicit H_∞ controllers for general rational systems of order less than or equal to 4 are obtained.

Working with unfixed model parameters have several attractive advantages. Firstly, given a parametric controller for a system with unfixed model parameters, only numerical evaluations of

these parameters are required to obtain a H_∞ controller for the system with fixed values of the parameters. This controller is obtained without requiring numeric optimization algorithms. This property can be interesting in the design of adaptive controllers since such symbolic controllers could easy be embedded because only evaluations of the closed-form expressions are required. Such a method is also interesting in a design stage of a project to quickly select a good architecture that can satisfy some given specifications.

In this paper, we propose to extend these techniques to certain time-delay systems, and to apply them to the stabilized mirror system which transfer function G is defined in Eq. 1.

Section 2 presents the control problem and classical results on H_∞ loop-shaping design. Section 3 gives useful results on the stabilization of an additive decomposition of a system. Section 4 shows how to link the controllers obtained in Section 3 with the studied robust control problem. Finally, Section 5 applies the developed approach to the stabilized mirror system presented above.

2. THE STANDARD H_∞ CONTROL PROBLEM FOR RATIONAL SYSTEMS

Let us recall standard results on robust control theory. We consider a *real rational system* $G_0 \in \mathbb{R}(s)$ and a *real rational controller* $K_0 \in \mathbb{R}(s)$ such that we have the closed-loop system defined in Figure 2. We then have

$$\begin{pmatrix} e_1 \\ y_1 \end{pmatrix} = \Pi(G_0, K_0) \begin{pmatrix} u_1 \\ u_2 \end{pmatrix},$$

where:

$$S_0 := (1 + G_0 K_0)^{-1},$$
$$\Pi(G_0, K_0) := \begin{pmatrix} S_0 & K_0 S_0 \\ G_0 S_0 & G_0 K_0 S_0 \end{pmatrix}.$$

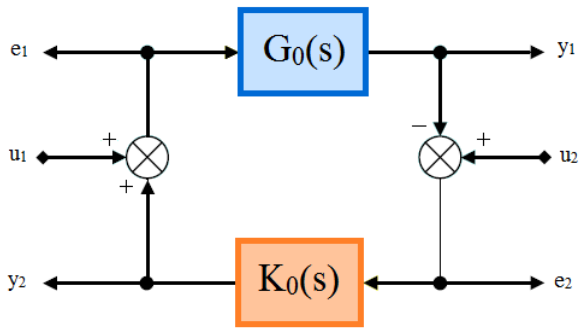

Figure 2 Control scheme

In the literature, a standard robust control problem can be stated as follows.

Robust Control Problem: Given $\gamma_0 > 0$, find a controller K_0 which stabilizes G_0 (i.e., such that the rational transfer functions S_0, $K_0 S_0$ and $G_0 S_0$ are proper and stable) and is such that

$$\|\Pi(G_0, K_0)\|_\infty < \gamma_0, \qquad \text{Eq. 2}$$

where $\|M\|_\infty := \sup_{\omega \in \mathbb{R}} \sqrt{\lambda_{\max}(M(j\omega)\, M(-j\omega)^T)}$ and $\lambda_{\max}$ is the largest real eigenvalue.

All of the entries of $\Pi(G_0, K_0)$ gives information about the closed-loop system:

- S_0 reflects the ability of y_1 to follow a reference u_2.
- $T_0 := G_0 K_0 S_0$ reflects the robustness to multiplicative model uncertainties of the closed-loop system.
- $K_0\, S_0$ yields the energy which is required to follow a reference u_2.
- $G_0\, S_0$ evaluates how the closed-loop system rejects disturbances acting on the input u_1 of G_0.

Hence, a controller K_0 satisfying Eq. 2 ensures a compromise between the performance of the closed-loop system and the robustness to model uncertainties. This compromise cannot be omitted since we have $S_0 + T_0 = 1$. For more details, see [4], [8], [9] and the references therein.

For linear finite-dimensional systems, Corollary 5.1 of [4] gives a numerical method to compute the minimal value of γ_0, denoted by γ_0^{opt}, and for $\gamma_0 > \gamma_0^{\text{opt}}$, a controller K_0 satisfying Eq. 2.

However, our approach considers a system with *unfixed model parameters*. As a consequence, *no numerical approach can be used here* and we shall use symbolic computation techniques. In [10], [11], [12], [13], these techniques were applied to H_∞ control in different situations. For SISO systems of order less than or equal to 4, [12] and [13] give explicit formulas for γ_0^{opt} and for $\gamma_0 > \gamma_0^{\text{opt}}$, a controller K_0 satisfying Eq. 2.

Since the stabilized mirror system involves a time-delay, i.e. a non rational system, we propose here to use an additive decomposition of G to deal with both the time-delay aspect and the unfixed parameters.

3. TIME-DELAY SYSTEMS AND ADDITIVE DECOMPOSITION

Let H_∞ be the Hardy algebra of holomorphic functions in $\mathbb{C}_+ := \{s \in \mathbb{C} \mid \mathrm{Re}(s) > 0\}$ which are bounded with respect to the norm $\|G\|_\infty = \sup_{s \in \mathbb{C}_+} |G(s)|$. Let RH_∞ be the subspace of H_∞ consisting of rational bounded holomorphic functions in $\mathbb{C}_+$. Let $F \in RH_\infty$ such that $F(0) \neq 0$. Let $\tau > 0$ and G be a time-delay system of the form:

$$G = \frac{F}{s} e^{-\tau s}.$$

We denote by $G_0 := \frac{F}{s} \in \mathbb{R}(s)$ the system G without time-delay, i.e. $\tau = 0$, and $\Delta := \left(\frac{1-e^{-\tau s}}{s}\right) F$. Since $\frac{1-e^{-\tau s}}{s} = \tau + O(s^2)$, $\frac{1-e^{-\tau s}}{s}$ has no poles in $\mathbb{C}_+$ and its H_∞ norm is equal to 1. Thus, we have $\Delta \in H_\infty$. Then, we can rewrite G as a sum of two systems:

$$G = G_0 - \Delta. \qquad \text{Eq. 3}$$

We then have the following theorem [14].

Theorem 1

Let $F \in RH_\infty$ such that $F(0) \neq 0$. Let $G_0 := \frac{F}{s} \in \mathbb{R}(s)$, $G = G_0\, e^{-\tau s}$ and $\Delta := \left(\frac{1-e^{-\tau s}}{s}\right) F \in H_\infty$. Let $K_0 \in \mathbb{R}(s)$ be a controller stabilizing G_0. Then, the following controller stabilizes G:

$$K(s) := \frac{K_0(s)}{1+\Delta(s)K_0(s)}.$$

Eq. 4

Theorem 1 gives a controller K stabilizing a time-delay system by means of a controller K_0 stabilizing a rational G_0, i.e. the system G without time-delay. This result can be depicted by the control scheme given in Figure 3. Furthermore, if the order of G_0 is less than or equal to 4, then [12] and [13] give explicit formulas for a H_∞ controller K_0 depending on the unfixed parameters of G_0. Combining these two facts, we can derive explicit controllers for the time-delay system G from the rational system G_0 of order less or equal to 4.

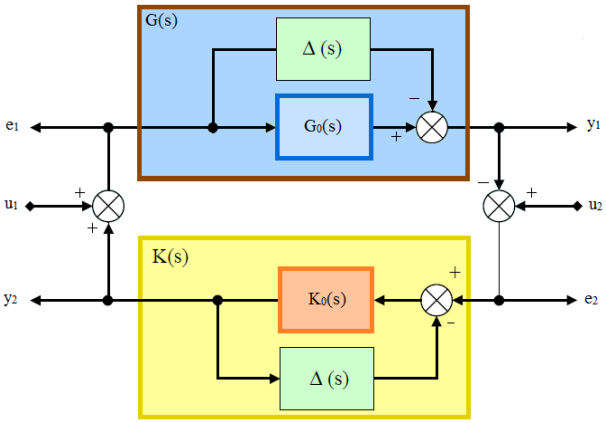

Figure 3 Control scheme of $G = G_0 - \Delta$

Even if K_0 stabilizes G_0 and satisfies Eq. 2, nothing can be said on $\|\Pi(G,K)\|_\infty$. Indeed, we have no precise measure on the loss on this H_∞ norm.

4. A SUB-OPTIMAL SOLUTION TO THE STANDARD H_∞ CONTROL PROBLEM APPLIED TO THE TIME-DELAY SYSTEM G

In this section, we consider F, G_0, G, Δ, K_0 and K as defined in Theorem 1. Let us also note:

$$\begin{cases} S_0 := (1+G_0K_0)^{-1}, \\ S := (1+GK)^{-1}, \\ T_0 := G_0\, K_0\, S_0, \\ T := GKS. \end{cases}$$

We seek for relations between $\Pi(G,K)$ and $\Pi(G_0,K_0)$. A particular one is given in the following theorem.

Theorem 2

Let $D := \begin{pmatrix} 1 & 0 \\ \Delta & 1 \end{pmatrix}$. We have:

$$\Pi(G,K) = D^{-1}\, \Pi(G_0,K_0)\, D.$$

Eq. 5

Furthermore, $D \in H_\infty$, $D^{-1} \in H_\infty$ *and* $\Pi(G,K) \in H_\infty$.

Proof Using Eq. 3 and Eq. 4, we have:

$$\begin{cases} S = (1+GK)^{-1} = \dfrac{1+\Delta\, K_0}{1+G_0K_0} = S_0 + \Delta S_0 K_0, \\ KS = K_0\, S_0, \\ G\, S = G_0\, S_0 + \Delta\, S_0\, (G_0K_0 - 1) - \Delta^2\, S_0\, K_0, \\ T = 1 - S = T_0 - \Delta\, S_0\, K_0. \end{cases}$$

Eq. 6

Eq. 6 yields:

$$\begin{aligned} \Pi(G,K) &= \begin{pmatrix} S & KS \\ GS & GKS \end{pmatrix} \\ &= \begin{pmatrix} 1 & 0 \\ -\Delta & 1 \end{pmatrix} \begin{pmatrix} S_0 & K_0S_0 \\ G_0S_0 & G_0K_0S_0 \end{pmatrix} \begin{pmatrix} 1 & 0 \\ \Delta & 1 \end{pmatrix} \\ &= \begin{pmatrix} 1 & 0 \\ -\Delta & 1 \end{pmatrix} \Pi(G_0,K_0) \begin{pmatrix} 1 & 0 \\ \Delta & 1 \end{pmatrix}. \end{aligned}$$

Denoting by $D := \begin{pmatrix} 1 & 0 \\ \Delta & 1 \end{pmatrix}$, and noticing that

$$D^{-1} = \begin{pmatrix} 1 & 0 \\ -\Delta & 1 \end{pmatrix},$$

we find that:

$$\Pi(G,K) = D^{-1}\, \Pi(G_0,K_0)\, D.$$

Eq. 7

Using $\Delta \in H_\infty$, we get $D \in H_\infty$ and $D^{-1} \in H_\infty$. Furthermore, $\Pi(G_0,K_0) \in H_\infty$ which implies $\Pi(G,K) \in H_\infty$ as the product of elements of H_∞.

□

Now, since $\Pi(G,K) \in H_\infty$, its H_∞ norm is finite and, when the model parameters are fixed to numerical values, an upper bound for it can be obtained using numerical techniques.

Note that we can compute an explicit bound on $\|\Pi(G,K)\|_\infty$. Let $D := \begin{pmatrix} 1 & 0 \\ \Delta & 1 \end{pmatrix} \in H_\infty$.Then, we have

$$\|\Pi(G,K)\|_\infty \leq \|\Pi(G_0,K_0)\|_\infty\, \|D\|_\infty^2,$$

and $\|D\|_\infty^2 = \sqrt{1 + \frac{1}{2}\|\Delta\|_\infty^2 + \sqrt{\left(1+\frac{1}{2}\|\Delta\|_\infty^2\right)^2 - 1}}.$

More details are given in Appendix.

For small order systems, $\|D\|_\infty^2$ (or a bound for it) can be made explicit (see, for instance [15], which gives a method to compute H_∞ norms by means of symbolic methods). For the stabilized mirror system, Δ has a particular shape and we can find an upper bound on $\|\Delta\|_\infty^2$. Indeed, let

$$R := \frac{\dfrac{s^2}{\omega_0^2} + 2\,\xi\,\dfrac{s}{\omega_0} + 1}{\dfrac{s^2}{\omega_1^2} + 2\,\xi\,\dfrac{s}{\omega_1} + 1},$$

and:

$$\begin{cases} \Omega := \dfrac{\omega}{\omega_1} \geq 0, \\ r := \dfrac{\omega_1}{\omega_0} \neq 1, \\ \delta := (r^2+1)^2 - 4r^2(2\xi^2-1)^2. \end{cases}$$

Then, we have

$$\|R\|_\infty := \begin{cases} 1 \quad if\ \xi \geq \dfrac{\sqrt{2}}{2},\ \ r < 1, \\ r^2 \quad if\ \xi \geq \dfrac{\sqrt{2}}{2},\ \ r > 1, \\ r\sqrt{\dfrac{1 - r^2 + \sqrt{\delta}}{r^2 - 1 + \sqrt{\delta}}} \quad if\ \xi < \dfrac{\sqrt{2}}{2},\ \ r < 1, \\ r\sqrt{\dfrac{r^2 - 1 + \sqrt{\delta}}{1 - r^2 + \sqrt{\delta}}} \quad if\ \xi < \dfrac{\sqrt{2}}{2},\ \ r > 1, \end{cases}$$

which implies:

$$\|\Delta\|_\infty \leq \tau\, g\, \|R\|_\infty.$$

A complete proof of this result is given in Appendix.

In practice, we notice that this bound is quite good for a system with the shape of a low-pass filter without resonance. For systems with highly resonating modes, this bound appears to be too large. In this case, it does not give us precise information about the feedback system.

Since the stabilized mirror system has highly resonating modes, we cannot rely on the above bound to characterize our control scheme. However, the following section shows that this approach appears to be quite effective in practice.

5. ADAPTIVE CONTROL OF THE STABILIZED MIRROR SYSTEM

5.1. Description of the system and assumptions

We now propose to apply the above approach to the stabilized mirror system which transfer function is given by:

$$G = \frac{g}{s}\left(\frac{\dfrac{s^2}{\omega_0^2} + 2\,\xi\,\dfrac{s}{\omega_0} + 1}{\dfrac{s^2}{\omega_1^2} + 2\,\xi\,\dfrac{s}{\omega_1} + 1}\right)\left(\frac{1}{Ts+1}\right) e^{-\tau s}.$$

Noting

$$\begin{cases} F := g\left(\dfrac{\dfrac{s^2}{\omega_0^2} + 2\,\xi\,\dfrac{s}{\omega_0} + 1}{\dfrac{s^2}{\omega_1^2} + 2\,\xi\,\dfrac{s}{\omega_1} + 1}\right)\left(\dfrac{1}{Ts+1}\right) \in RH_\infty, \\ G_0 := \dfrac{F(s)}{s} \in \mathbb{R}(s), \\ \Delta := \left(\dfrac{1 - e^{-\tau s}}{s}\right) F(s) \in H_\infty, \end{cases}$$

this system G can be decomposed as:

$$G = G_0 - \Delta.$$

In what follows, we fix the parameters to the following values:

$$\omega_0 := 1,\ \ T := 1,\ \ \ \xi := 10^{-2},\ \ \ g := 10^{-3},\ \ \ \tau := 1.$$

Furthermore, we assume that *the natural modal frequency* ω_1 *can slowly vary* and it is considered as an unfixed model parameter. Moreover, we assume that ω_1 satisfies the following assumption:

$$\omega_1 > 1.$$

Figure 4 represents the Bode diagram of G while the frequency ω_1 varies in the following set:

$$\Omega_\star := \{1.1, 1.47, 1.95, 2.42, 2.89, 3.37, 3.84, 4.3158\ 4.79, 5.26, 5.74, 6.21, 6.68, 7.16, 7.63, 8.11,\ 8.58, 9.05, 9.53, 10\}.$$

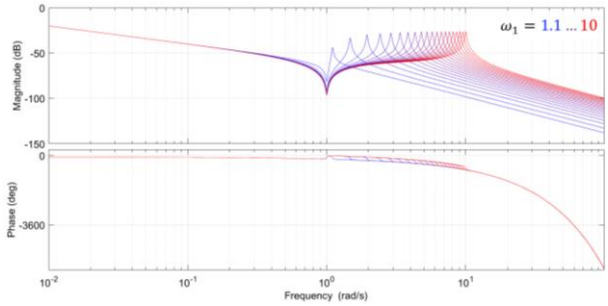

Figure 4 Bode plot of the physical system G while $\omega_1 \in \Omega_\star$

Given this parametric system, we seek for a controller which provides a good compromise between performance and robustness as well as a way to control this compromise. To do that, we use some concepts of loop-shaping design [4], [8], [6].

5.2. Loop-shaping design

In practice, engineers want to ensure certain performance and robustness properties for a given configuration. For rational systems, [8] provides the following relations between γ_0, satisfying $\|\Pi(G_0, K_0)\|_\infty < \gamma_0$, and m_G and m_ϕ defined by

$$\begin{cases} \mathrm{M}_G(G_0, K_0) \geq m_G(\gamma_0) := \dfrac{1 + \gamma_0^{-1}}{1 - \gamma_0^{-1}}, \\ \mathrm{M}_\phi(G_0, K_0) \geq m_\phi(\gamma_0) := 2\arcsin(\gamma_0^{-1}), \end{cases} \qquad \text{Eq. 8}$$

where $\mathrm{M}_G(G_0, K_0)$ (resp. $\mathrm{M}_\phi(G_0, K_0)$) represents the *gain* (resp. *phase*) *margin* of the open-loop system.

Based on the concept of *loop-shaping* (see [6], [8]), let us introduce a tuning parameter $w > 0$ and let us define the *fictive plant* P by

$$P := w\, G,$$

where G, defined in Eq. 1 is a model of the *physical plant*. We also denote the static gain of P by:

$$p := w\, g.$$

Since $P = w\, G_0\, e^{-\tau s}$, then we can define

$$P_0 := w\, G_0,$$

such that we have:

$$P = P_0\, e^{-\tau s}.$$

Hence, P (resp. P_0) is just obtained by substituting g by p into G (resp. G_0). Let us also denote by θ the unfixed model parameters of the system:

$$\theta := (p,\ \omega_1).$$

Since P_0 is a rational SISO system of order 4, using [13], we can explicitly compute a controller C_0

stabilizing P_0 and the optimal upper bound γ_0^{opt} on $\|\Pi(P_0, C_0)\|$, i.e.

$$\gamma_0^{opt}(\theta) := \min_{C_0} \{\gamma_0 \mid \|\Pi(P_0, C_0)\|_\infty \leq \gamma_0\}, \qquad \text{Eq. 9}$$

in terms of θ. $\gamma_0^{\text{opt}}(\theta)$ is ploted in Figure 5.

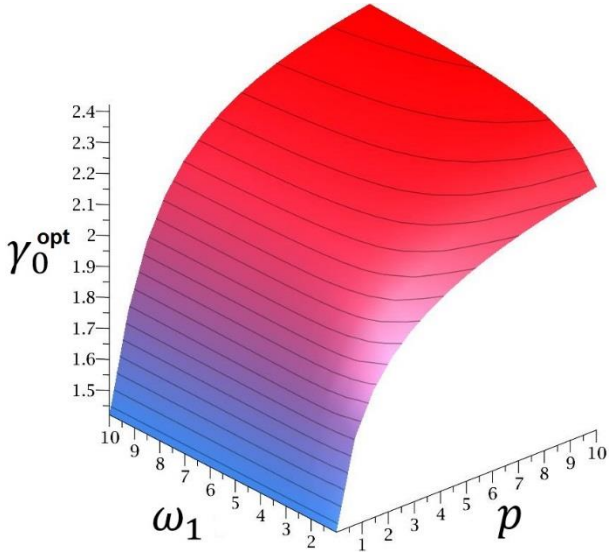

Figure 5 Plot of $\gamma_0^{opt}(p, \omega_1)$

Therefore, for all values of θ, m_G and m_ϕ of $C_0\, P_0$ are explicitly known (see Eq. 8).

By Theorem 1, if C_0 stabilizes P_0, then the controller $C := \frac{C_0}{1+C_0\,\Delta}$ stabilizes the fictive plant P. Since we have

$$C\,P = \left(\frac{K}{w}\right)(G\,w) = K\,G,$$

the controller $K := w\,C$ stabilizes G.

Note that the weight w preserves the norms $\left\|\frac{1}{1+PC}\right\|_\infty$ and $\left\|\frac{PC}{1+PC}\right\|_\infty$ but we have $\left\|\frac{K}{1+GK}\right\|_\infty = w\left\|\frac{C}{1+PC}\right\|_\infty$ and $\left\|\frac{G}{1+GK}\right\|_\infty = \frac{1}{w}\left\|\frac{P}{1+PC}\right\|_\infty$ (see [8] for more details). In other words, only open-loop properties are preserved from the fictive plant to the physical system. But w provides a degree of freedom that can be used to shape the open-loop transfer. More precisely, in the next sections, we will use w to fix m_G and m_ϕ for $C_0 P_0$.

5.3. Loop-shaping design for a particular time-delay system

In this sub-section, we set the particular value

$$\bar{\omega}_1 := 2,$$

for ω_1 while the other parameters are still fixed to the following values:

$$\omega_0 := 1, \quad T := 1, \quad \xi := 10^{-2}, \quad g := 10^{-3}, \quad \tau := 1.$$

Note that w still remains unfixed in this case. Through trial and error and using a Black-Nichols plot of GK (see Figure 6), we set the value

$$w = \bar{w} := 564.7$$

such that the stability margins M_G and M_ϕ of the open-loop transfer GK are sufficiently large:

$$\begin{cases} \mathrm{M}_G(G,K) = 10.7\ \mathrm{dB}, \\ \mathrm{M}_\phi(G,K) = 67.6°. \end{cases}$$

We note that the phase margin is obtained at the frequency $0.283\ \mathrm{rad.s^{-1}}$, corresponding to the bandwidth of the open-loop transfer.

Given this weight w, the corresponding value of $\gamma_0^{\text{opt}}(\bar{w}g, \omega_1)$ is 1.7. Hence, we have:

$$\|\Pi(P_0, C_0)\|_\infty \leq 1.7.$$

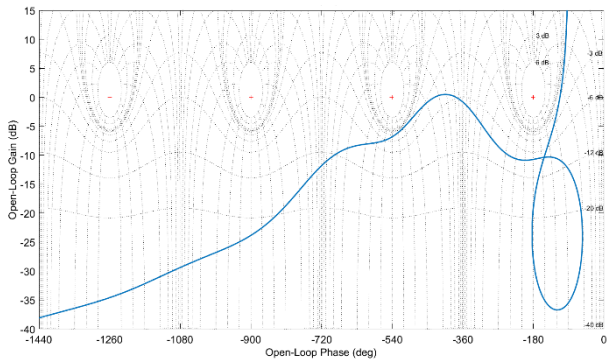

Figure 6 Black-Nichols plot of GK with $\omega_1 = 2$.

5.4. An explicit controller stabilizing G

Let us now suppose that $\omega_1 > 1$ is unfixed. Let $\bar{\gamma}_0 > 0$ be a chosen numerical value for γ_0^{opt} defined in Eq. 9. We seek for a method to ensure that $\gamma_0^{\text{opt}}(p, \omega_1) \simeq \bar{\gamma}_0$ in the neighborhood of $\bar{\omega}_1$.

Section 5.2 has shown that for $\omega_1 = \bar{\omega}_1$, the value of $\gamma_0^{\text{opt}} = 1.7$ gives confortable stability margins for GK. Hence, let us choose $\bar{\gamma}_0 = 1.7$.

Intersecting the surface of Figure 5 with the plane $\gamma_0^{\text{opt}} = \bar{\gamma}_0$, we obtain the blue curve of Figure 7.

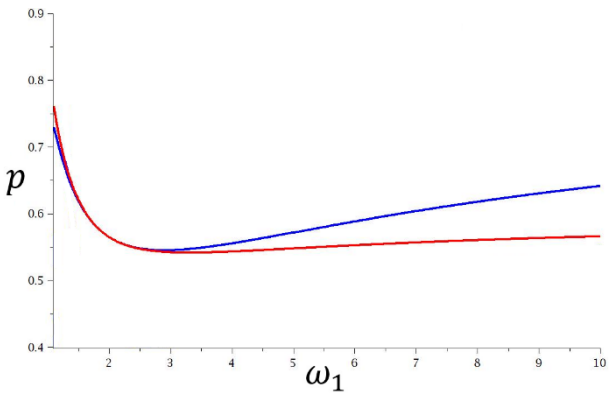

Figure 7 Blue: $\gamma_0^{\text{opt}}(\mathrm{p}, \omega_1) = 1.7$ – Red: $p = p_{\bar{\gamma}_0}(\omega_1)$.

Following the work of [13], we can locally approximate the curve $\gamma_0^{\text{opt}}(p, \omega_1) = \bar{\gamma}_0$ by a function of the form:

$$p = p_{\bar{\gamma}_0}(\omega_1).$$

This approximation is done around the point

$$\omega_1 = \bar{\omega}_1, \;\; p = \bar{w}g = 0.5647,$$

and is given by the following explicit formula:

$$p_{\overline{\gamma_0}}(\omega_1) := 0.5959 + \frac{0.5968}{\omega_1^2} - \frac{0.3607}{\omega_1}.$$

The curve $p = p_{\overline{\gamma_0}}(\omega_1)$ is drawn in red in Figure 7.

Also, we can verify that γ_0^{opt} remains close to $\overline{\gamma_0}$ by evaluating the symbolic expression $\gamma_0^{\text{opt}}(p_{\overline{\gamma_0}}(\omega_1), \omega_1)$, which is a function of the unique variable ω_1 (see Figure 8). Note that γ_0^{opt} is exactly $\overline{\gamma_0}$ at $\omega_1 = \bar{\omega}_1$ and stays close to this value in the neighborhood this working point.

Given $\gamma > \gamma_0^{\text{opt}}(p_{\overline{\gamma_0}}(\omega_1), \omega_1)$, we can compute an explicit adaptive H_∞ controller $C_0(s, \omega_1)$ stabilizing $P_0(s, \omega_1)$ depending on the unfixed parameter ω_1 and ensuring γ_0^{opt} being close to $\overline{\gamma_0}$ [13]. Then, using Theorem 1,

$$C(s, \omega_1) = \frac{C_0(s, \omega_1)}{1 + C_0(s, \omega_1)\Delta(s, \omega_1)}$$

stabilizes P. Choosing the weight

$$w = w_{\overline{\gamma_0}}(\omega_1) := p_{\overline{\gamma_0}}(\omega_1)/g,$$

we deduce that the following controller

$$K(s, \omega_1) := w_{\overline{\gamma_0}}(\omega_1) C(s, \omega_1) = \frac{w_{\overline{\gamma_0}}(\omega_1)\, C_0(s, \omega_1)}{1 + C_0(s, \omega_1)\Delta(s, \omega_1)}$$

stabilizes $G(s, \omega_1)$.

The values of the weight $w_{\overline{\gamma_0}}(\omega_1)$ taken for $\omega_1 \in \Omega_\star$ are ploted in Figure 9.

This loop-shaping design process is summarized in Figure 10.

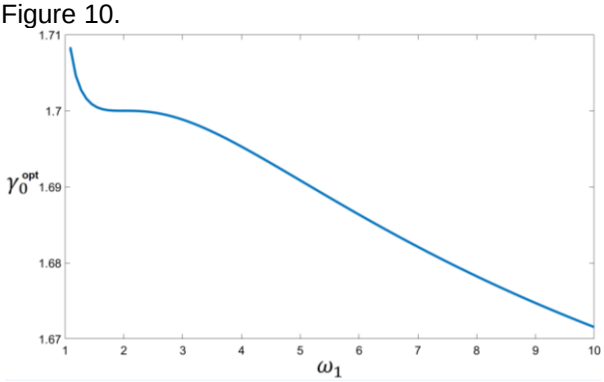

Figure 8 Evolution of $\gamma_0^{opt}(p_{\overline{\gamma_0}}(\omega_1), \omega_1)$

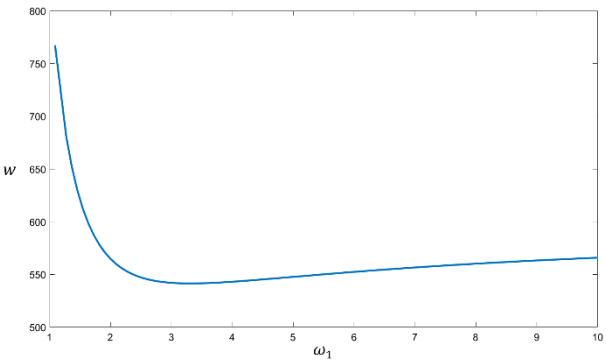

Figure 9 Plot of $w_{\overline{\gamma_0}}(\omega_1)$

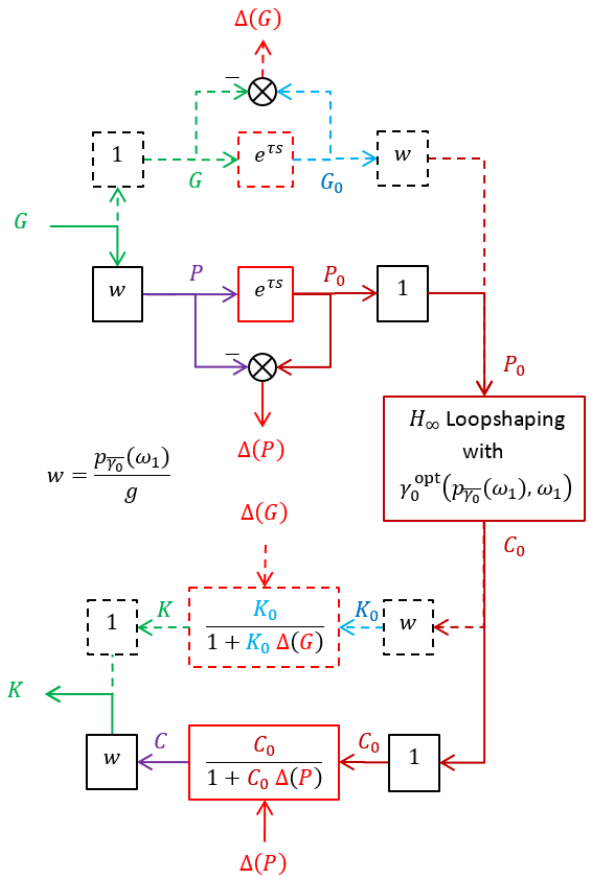

Figure 10 Loop-shaping process

Remark 1.

The explicit expressions of $\gamma_0^{\text{opt}}(\theta)$, $C_0(\theta)$ and $C(\theta)$ are too long to be displayed here. Again, we refer to [13] *for their constructions.*

The Bode plot of $K(s, \omega_1)$, evaluated at different $\omega_1 \in \Omega_\star$, is given in Figure 11. In green, the nominal controller is represented, i.e. the controller $K(s, \omega_1)$ obtained for $\omega_1 = \bar{\omega}_1 = 2$. We can see that $K(s, \omega_1)$ has a low gain at the frequency of the mode. Since $K(s, \omega_1)$ explicitly depends on the unfixed model parameter ω_1, this rejector automatically changes with ω_1 in a neighborhood of $\bar{\omega}_1 = 2$ without requiring optimization algorithms.

5.5. Open-loop characteristics

The Bode plot of the open-loop is given in Figure 13 while its Black-Nichols plot is given in Figure 14. On Figure 13, we can see that for $\omega_1 = 1.1$, the bandwith is large, and for other values in $\Omega_\star$, the bandwidth is close to 0.3. Also, Figure 14 is particularly interesting since we can see the conservation of the stability margins while ω_1 varies: for $1.1 < \omega_1 < 10$, we have:

$$\mathrm{M}_G(G, K) > 9 \text{ dB},$$
$$\mathrm{M}_\phi(G, K) > 70°.$$

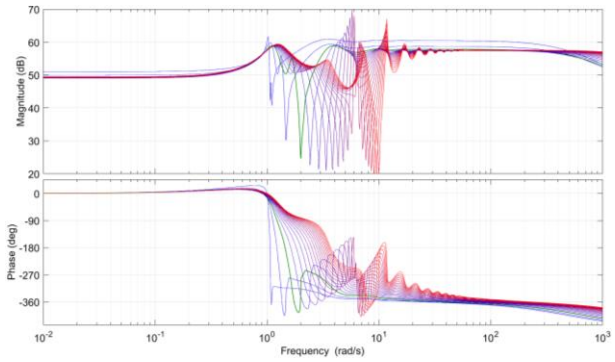

Figure 11 Bode plot of $K(\omega_1)$

Remark 2.

Consider a nominal controller K of G obtained for $\omega_1 = 2$ (see the green curve of Figure 11). In Figure 12, we plot the Black-Nichols diagram of the open-loop GK while G varies for particular values of ω_1. As we can see, if K is fixed and ω_1 varies, the closed-loop system can become unstable, which justifies our adaptive approach for which the closed-system remains stable since the controller $K(s, \omega_1)$ automatically changes with the frequency ω_1.

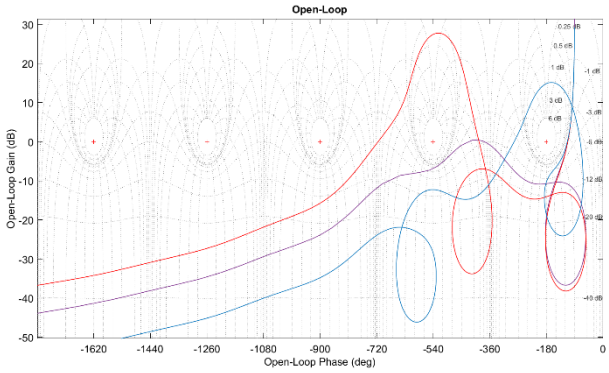

Figure 12 Black-Nichols plot of GK where K is fixed and set at $\omega_1 = 2$ but P varies with ω_1.
Blue: $\omega_1 = 1.1$ (unstable) – Violet: $\omega_1 = 2$ (stable) – Red: $\omega_1 = 3$ (unstable

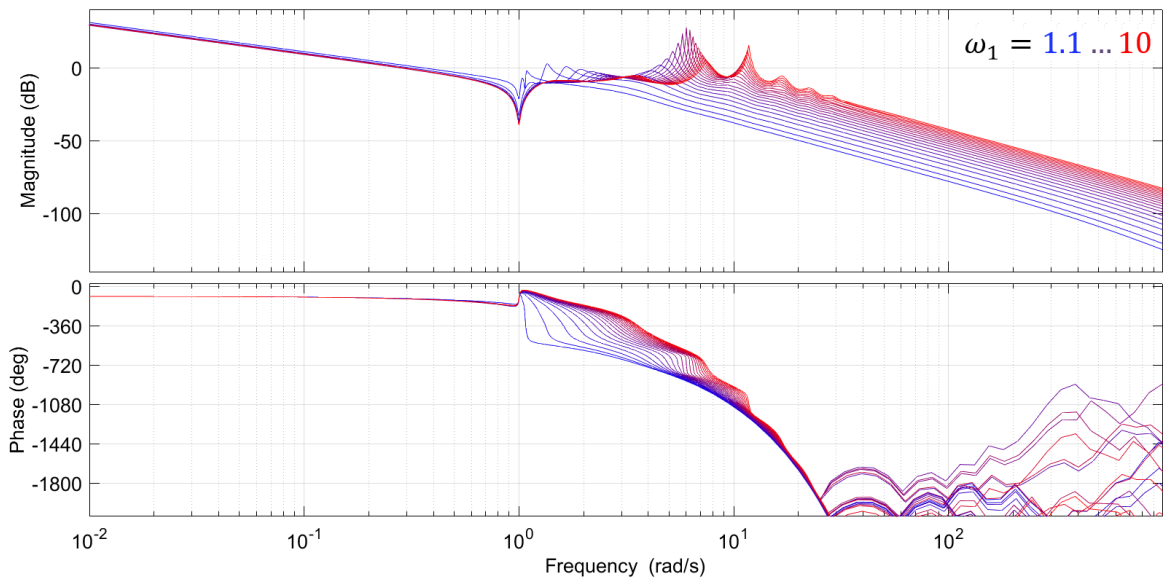

Figure 13 Bode plot of the open-loop GK

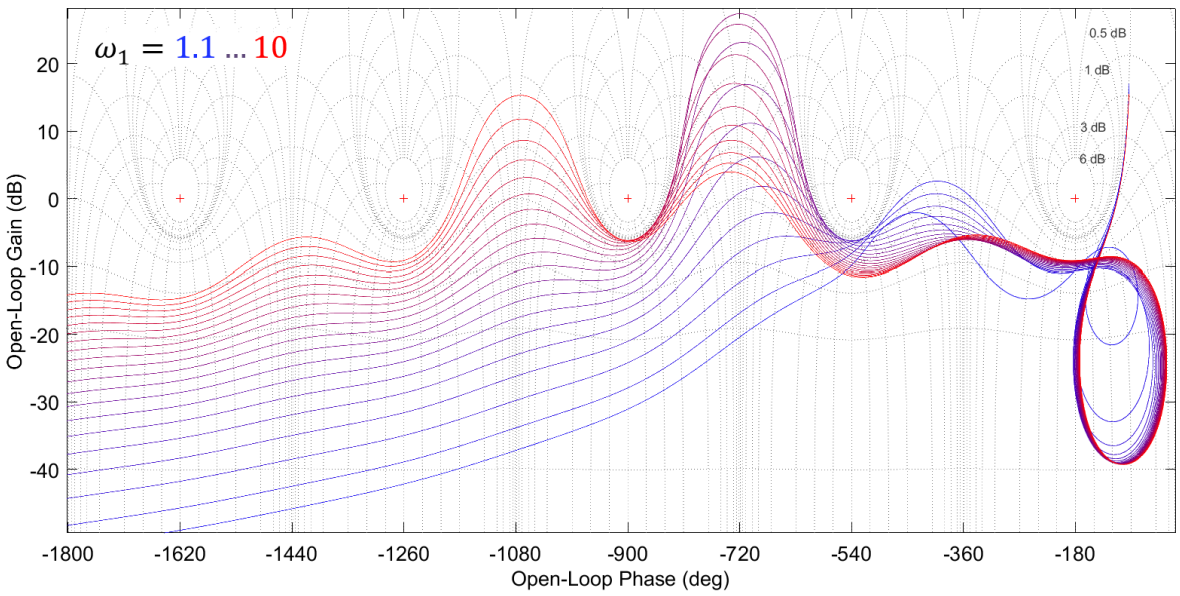

Figure 14 Black-Nichols plot of the open-loop GK

5.6. Closed-loop characteristics

To finish, we point out interesting characteristics of the closed-loop system. In section 2, we recalled the meaning of each component of $\Pi(G,K)$. The Bode plots of each transfer function of $\Pi(G,K)$ are given in Figure 15, Figure 16, Figure 17 and Figure 18. We also give step response of T in Figure 19 (i.e. the response of the output to a step as a reference input), and the step response of GS in Figure 20 (i.e. the response of the output to a torque disturbance defined by a step). On these plots, we can notice a few interesting facts.

First of all, we have $20\log(\|T\|_\infty) \leq 0$ dB for all $\omega_1 \in \Omega_\star$, which ensures a good robustness with respect to model uncertainties characterized by multiplicative errors [8], [6].

Also, we have $20\log(\|S\|_\infty) < 6$ dB for all $\omega_1 \in \Omega_\star$, which ensures a good reference tracking without huge overshoots of the output.

Besides, we note some quite high gains in $\|GS\|_\infty$ due to the mechanical structure of the system. Indeed, since the mechanical system G has highly resonating modes, they are still present in GS and they cannot be attenuated using K without degrading the transfer S (i.e. the overall performance). Thus, we can see some oscillations in the step response of GS (see Figure 20). By adding integrators in K for low frequencies, this step response tends to zero (which has not been done here).

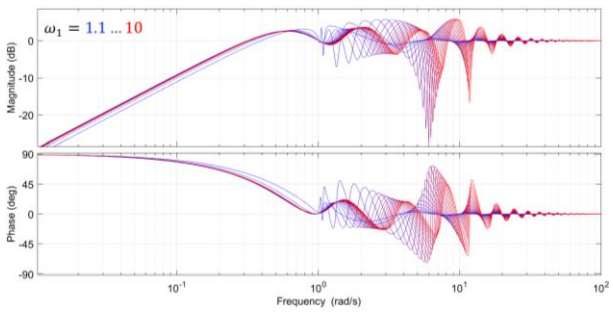

Figure 15 Sensitivity transfer function S

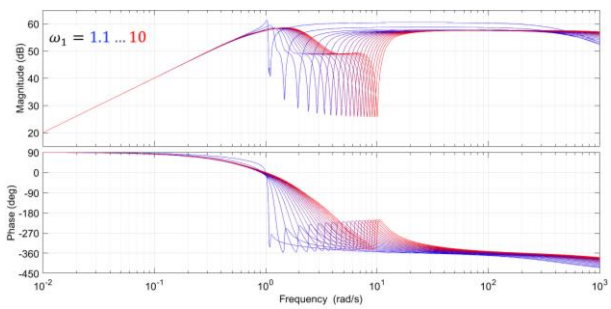

Figure 16 Transfer function KS

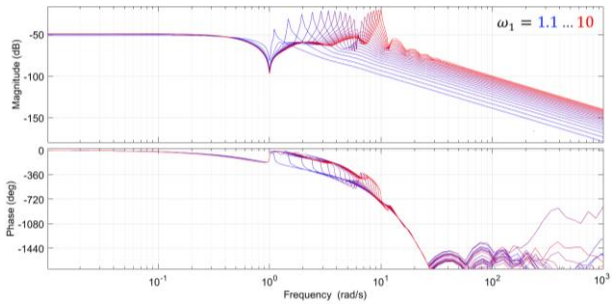

Figure 17 Transfer function GS

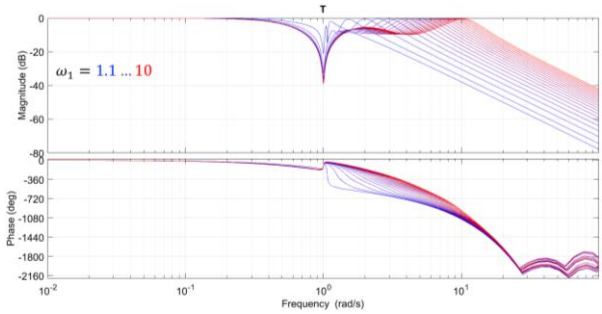

Figure 18 Transfer function T

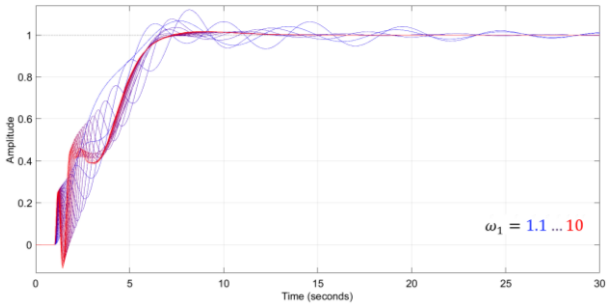

Figure 19 Step response of T

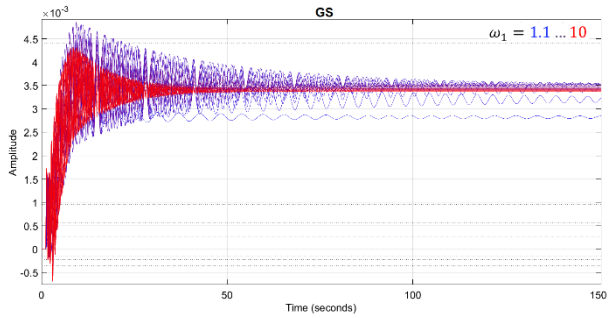

Figure 20 Step response of GS

6. CONCLUSION

In this paper, we have proposed a method to compute an explicit H_∞ controller of a fourth order time-delay system based on an additive decomposition of the system. By controlling the H_∞ criterion of the non-delayed system (i.e. the system G with $\tau = 0$), this explicit controller naturally achieves a compromise between the performance and the robustness. This controller is particularly interesting for the control of an optro-mechanical structure with highly resonating and varying modes such as the stabilized mirror system.

Future work will focus on finding ways to explicitly characterize the properties of this controller by means of the H_∞ norm of $\Pi(G,K)$ or one of its entries. Also, real-time parameter estimation techniques are now studied to obtain an embeddable adaptive controller. Finally, this class of systems with a varying damping will be considered in future publications.

7. APPENDIX

In this appendix, we give an explicit upper bound for $\|\Pi(G,K)\|_\infty$ where G is defined in Eq. 1.

First, from Eq 5, we have:

$$\|\Pi(G,K)\|_\infty \leq \|D^{-1}\|_\infty \|\Pi(G_0,K_0)\|_\infty \, \|D\|_\infty.$$

Now, let us compute the characteristic polynomial of $D(j\,\omega)\,D^\star(j\,\omega)$:

$$\begin{aligned} h_D &\coloneqq \det\begin{pmatrix} 1-\lambda & \Delta^\star(j\,\omega) \\ \Delta(j\,\omega) & \Delta(j\,\omega)\Delta^\star(j\,\omega)+1-\lambda \end{pmatrix}, \\ &= \lambda^2 - (\Delta(j\,\omega)\Delta^\star(j\,\omega)+2)\lambda + 1. \end{aligned}$$

By replacing $\Delta(j\,\omega)$ by $-\Delta(j\,\omega)$, we note that the characteristic polynomial of $D(j\,\omega)^{-1}D^{-1^\star}(j\,\omega)$ also gives h_D. Hence, we have

$$\|D^{-1}\|_\infty = \|D\|_\infty,$$

which yields:

$$\|\Pi(G,K)\|_\infty \leq \|\Pi(G_0,K_0)\|_\infty \, \|D\|_\infty^2.$$

Furthermore, with $\epsilon \in \{-1,1\}$, the roots of h_D are given by:

$$\lambda_\epsilon \coloneqq 1 + \tfrac{1}{2}|\Delta(j\,\omega)|^2 + \epsilon\sqrt{\left(1+\tfrac{1}{2}|\Delta(j\,\omega)|^2\right)^2 - 1}.$$

Also, for $\omega \geq 0$, we have $|\Delta(j\,\omega)|^2 \geq 0$, and thus we get $\lambda_1(\omega) \geq \lambda_{-1}(\omega)$. Denoting by ω_m the frequency at which $|\Delta(j\,\omega)|$ is maximal, we then have:

$$\|\Delta\|_\infty = |\Delta(j\,\omega_m)|.$$

Thus, we have:

$$\|D\|_\infty = \sqrt{1+\frac{1}{2}\|\Delta\|_\infty^2 + \sqrt{\left(1+\frac{1}{2}\|\Delta\|_\infty^2\right)^2 - 1}}.$$

Now, we propose to find an explicit upper bound for $\|\Delta\|_\infty$. We assume that the parameters respect some assumptions:

$$0 < \xi \leq 1, \quad T > 0, \quad \tau > 0, \quad \omega_0 > 0, \quad \omega_1 > \omega_0.$$

For all $\omega \in \mathbb{R}, \omega > 0$, we have:

$$|\Delta(j\,\omega)| \coloneqq \left|\frac{1-e^{-\tau j\,\omega}}{j\,\omega}\right| |F(j\omega)|.$$

Furthermore, we have:

$$\begin{aligned} \left|\frac{1-e^{-j\tau\omega}}{j\omega}\right| &= \frac{1}{\omega}|1-(\cos(\tau\omega)-j\sin(\tau\omega))| \\ &= \frac{\sqrt{2}}{\omega}\sqrt{1-\cos(\tau\omega)} \\ &= \frac{\sqrt{2}}{\omega}\sqrt{2\sin^2\left(\frac{\tau\omega}{2}\right)} \\ &= \tau\left|\mathrm{sin}_c\left(\frac{\tau\omega}{2}\right)\right|, \end{aligned}$$

where $\mathrm{sin}_c(x) \coloneqq \frac{\sin(x)}{x}$ denotes the cardinal sinus function. sin_c admits 1 as its maximum at zero. Thus, we have

$$\|\Delta\|_\infty = \left\|\left(\frac{1-e^{-\tau s}}{s}\right)F\right\|_\infty \leq \left\|\left(\frac{1-e^{-\tau s}}{s}\right)\right\|_\infty \|F\|_\infty,$$

which yields:

$$\|\Delta\|_\infty \leq \tau\|F\|_\infty.$$

However, note that $\left\|\left(\frac{1}{1+Ts}\right)\right\|_\infty = 1$. Then, by denoting by

$$R \coloneqq \frac{\frac{s^2}{\omega_0^2} + 2\,\xi\,\frac{s}{\omega_0} + 1}{\frac{s^2}{\omega_1^2} + 2\,\xi\,\frac{s}{\omega_1} + 1},$$

we have:

$$\|F\|_\infty \leq g\,\|R\|_\infty.$$

Thus, it only remains to compute $\|R\|_\infty$. Performing the change of variable $\omega = \Omega\omega_1$ and using $r \coloneqq \frac{\omega_1}{\omega_0}$, we obtain:

$$\bar{R}(j\Omega) \coloneqq \frac{1 - r^2\Omega^2 + 2\,\xi\,r\,\Omega\,j}{1 - \Omega^2 + 2\,\xi\,\Omega\,j}.$$

By doing such a change of variable, the H_∞ norm remains unchanged:

$$\|R\|_\infty = \max_{\omega\in\mathbb{R}}|R(j\omega)| = \max_{\Omega\in\mathbb{R}}|\bar{R}(j\Omega)| = \|\bar{R}\|_\infty.$$

Hence, we prefer to work with variables Ω and r since we are working with only 2 parameters (while R as 3 parameters). Let us note:

$$P \coloneqq \Omega\,(\,r^2(2\,\xi^2-1)\,\Omega^4 + (r^2+1)\Omega^2 + 2\,\xi^2 - 1).$$

Then, we have:

$$\frac{\partial|\bar{R}(j\Omega)|^2}{\partial\Omega} = \frac{4\,(r-1)\,(r+1)\,P(\Omega,r,\xi)}{((1-\Omega)^2 + 4\,\xi^2\Omega^2)^2}.$$

Since $\xi > 0$, the denominator of $\frac{\partial|\bar{R}(j\Omega)|^2}{\partial\Omega}$ cannot vanish and is strictly positive. Assuming $r > 1$, $|\bar{R}(j\Omega)|$ is extremal if and only if P vanishes. P is a product of Ω and a polynomial of degree 2 in Ω^2, which roots can be found by radicals. Noting $\Omega_0 \coloneqq 0$, $\epsilon \in \{-1,1\}$ and

$$\delta(r,\xi) \coloneqq (r^2+1)^2 - 4\,r^2(2\,\xi^2-1)^2,$$

$$\Omega_\epsilon \coloneqq \sqrt{\frac{-(r^2+1) + \epsilon\sqrt{\delta(r,\xi)}}{2\,r^2(2\,\xi^2-1)}},$$

the roots of P are:

$$E_\Omega := \{\Omega \,|P(\Omega) = 0\} := \{\Omega_0, \Omega_{-1}, \Omega_1, -\Omega_{-1}, -\Omega_1\}.$$

The roots of P define the frequencies Ω where $|\bar{R}(j\Omega)|$ admits an extremum. It remains to determine which $\Omega \in E_\Omega$ corresponds to the maximum of $|\bar{R}(j\Omega)|$. This maximum can change while the parameters vary.

When P admits a root of multiplicity 2 or more, its discriminant vanishes. This exactly corresponds to the location where two distinct Ω_i are equal. For more details, see [16]**.** The discriminant of P is defined by:

$$\delta_P := \left(4\, r\, (2\,\xi^2 - 1)\, \delta(r,\xi)\right)^2.$$

Basic calculations show that:

$$\delta_P = 0 \;\Leftrightarrow\; 2\,\xi^2 - 1 = 0 \;\Leftrightarrow\; \xi = \xi_c := \frac{\sqrt{2}}{2}.$$

Thus, we can split the parameter space into cells where the number of real roots of P is constant as shown in Figure 21.

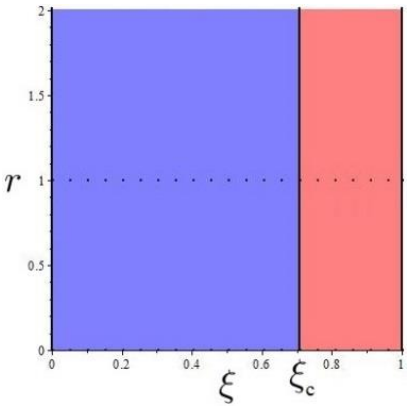

Figure 21 Cell decomposition of the parameter space

By evaluation of the closed form expressions Ω_ϵ at a particular point of each cell, we show that:

- If $\xi > \xi_c$ (red cell), then $\Omega_0 = 0$ is the only real root of P.
- If $\xi < \xi_c$ (blue cell), then P has 5 real roots and $\Omega_1 > \Omega_{-1} > \Omega_0 > -\Omega_{-1} > -\Omega_1$.

We also point out that the have:

- $\lim\limits_{\Omega \to 0} |F_i(j\Omega)| = 1,$
- $\lim\limits_{\Omega \to +\infty} |F_i(j\Omega)| = r^2.$

Given the above remarks, we distinguish two cases.

Case 1: $\boldsymbol{\xi > \xi_c}$. $|\bar{R}(j\Omega)|$ admits a unique extrema at $\Omega_0 = 0$. Thus, we have:

$$\xi > \xi_c, \qquad \|R\|_\infty := \begin{cases} 1 & \text{if } r < 1, \\ r^2 & \text{if } r > 1. \end{cases}$$

Case 2: $\boldsymbol{\xi < \xi_c}$. First, we notice that $|\bar{R}(j\Omega)|$ decreases in the neighbourhood of 0 if $r > 1$, and increases otherwise. Furthermore, remind that in this case, we have $\Omega_1 > \Omega_{-1} > \Omega_0$. Thus, the variations of $|\bar{R}(j\Omega)|$ are then given by Figure 22 and we deduce its maximum value.

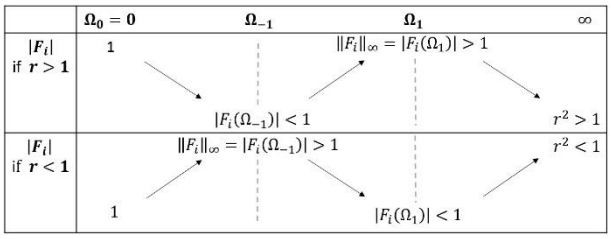

Figure 22 Variations of $|\bar{R}(j\Omega)|$ while $\boldsymbol{\xi < \xi_c}$

Substituing the symbolic expressions of Ω_1 and Ω_{-1} into $|\bar{R}(j\Omega)|$, and simplifying the obtained expressions (for instance using a symbolic computing environment such as *Maple*) gives

$$\|R\|_\infty := \begin{cases} 1 & \text{if } \xi \geq \dfrac{\sqrt{2}}{2},\ r < 1, \\ r^2 & \text{if } \xi \geq \dfrac{\sqrt{2}}{2},\ r > 1, \\ r\sqrt{\dfrac{1 - r^2 + \sqrt{\delta}}{r^2 - 1 + \sqrt{\delta}}} & \text{if } \xi < \dfrac{\sqrt{2}}{2},\ r < 1, \\ r\sqrt{\dfrac{r^2 - 1 + \sqrt{\delta}}{1 - r^2 + \sqrt{\delta}}} & \text{if } \xi < \dfrac{\sqrt{2}}{2},\ r > 1, \end{cases}$$

where:

$$\begin{cases} \Omega := \dfrac{\omega}{\omega_1} \geq 0, \\ r := \dfrac{\omega_1}{\omega_0} \neq 1, \\ \delta := (r^2 + 1)^2 - 4r^2(2\xi^2 - 1)^2. \end{cases}$$

From this symbolic expression, we deduce an upper bound on $\|\Pi(G,K)\|_\infty$ as explained in Section 4.

REFERENCES

[1] P. J. Kennedy and R. Kennedy, Line of Sight Stabilization Primer, Electronic book, 2013.

[2] M. K. Masten, Inertially stabilized platforms for optical imaging systems, IEEE Control Systems, 2008, p. 47–64.

[3] J. M. Hilker, Inertially stabilized platform technology: concepts and principles, IEEE Control Systems, 2008.

[4] K. Glover and D. McFarlane, Robust stabilization of normalized coprime factors: An explicit H∞ solution, ACC, 1988.

[5] P. Coustal, Contribution au contrôle robuste des structures flexibles, Doct. diss., 1997.

[6] P. Feyel, Loop-shaping robust control, John Wiley & Sons, 2013.

[7] S. Hirwa, Méthodes de commande avancées appliquées aux viseurs, Doct. diss., 2013.

[8] G. Vinnicombe, Uncertainty and feedback-loop-shaping and the μ-gap metric, Imperial college Press, 2001.

[9] K. Zhou, J. C. Doyle and K. Glover, Robust

and Optimal Control, Prentice-Hall, Inc, 1996.

[10] M. Kanno and S. Hara, Symbolic-numeric hybrid optimization for plant/controller integrated design in H∞ loop-shaping design, Journal Math-for-Industry, 2012, p. 135–140.

[11] G. Rance, Y. Bouzidi, A. Quadrat and A. Quadrat, A symbolic-numeric method for the parametric H∞ loop-shaping design problem, 22nd International Symposium on Mathematical Theory of Networks and Systems, 2016, p. 574–581.

[12] G. Rance, Y. Bouzidi, A. Quadrat and A. Quadrat, Explicit H∞ controllers for 1st to 3rd order single-input single-ouput systems with parameters, 20th IFAC World Congress, 2017, p. 721–726.

[13] G. Rance, Y. Bouzidi, A. Quadrat, A. Quadrat and F. Rouillier, Explicit H∞ controllers for 4th order single-input single-ouput systems with parameters and their application to the two mass-spring system with damping, 20th IFAC World Congress, 2017, p. 727–732.

[14] A. Quadrat and A. Quadrat, Delay effects in visual tracking problems for an optronic sighting system, Low-Complexity Controllers for Time-Delay Systems, Springer, 2014, p. 77–92.

[15] M. Kanno and M. C. Smith, Validated numerical computation of the L∞-norm for linear dynamical systems, Journal of Symbolic Computation, 2006, p. 697–707.

[16] D. Lazard and F. Rouillier, Solving parametric polynomial systems, vol. 42, Journal of Symbolic Computation, 2007, p. 636–667.